Mineralogical Magazine, October 1999, Vol. 63(5), pp. 703–722

Petrology and geochemistry of xenoliths in lamprophyres from the Deccan Traps: implications for the nature of the deep crust boundary in western India

A. G. DESSAI[1] AND O. VASELLI[2]

[1] Department of Geology, Goa University, Taleigao Plateau, Goa 403 206, India
[2] Department of Earth Sciences, University of Florence, 50121 Florence, via G. la Pira, 4, Italy

ABSTRACT

Alkaline lamprophyre intrusives from the western Deccan Traps (Murud-Janjira, south of Bombay) host rare lithospheric xenoliths and megacrysts. The xenolith suite consists of clinopyroxenites and granulites which show eclogitic affinities. The former have transitional (porphyroclastic to equigranular) textures whereas the latter are porphyroclastic, xenomorphic to meta-igneous. The textural features provide evidence of ductile-brittle deformation. The protoliths of the pyroxenite and granulite xenoliths were formed as cumulates of alkaline and sub-alkaline magmas respectively.

Mineral chemistry and geochemical data for the xenoliths bear testimony to the metasomatized nature of the deep crust. The xenolith data coupled with the geophysical evidence indicate that the lower crust beneath Murud-Janjira is dominated by mafic granulites and pyroxenites. The latter have under- and intra-plated the continental crust beneath the region.

KEYWORDS: xenoliths, lamprophyres, Deccan Traps, deep crust boundary.

Introduction

LITHOSPHERIC xenoliths in alkali basalts and kimberlites have attained considerable importance in recent years as windows to the petrological and geochemical characteristics of the lower crust and upper mantle. Accidental lithospheric xenoliths represent pristine samples which can provide information on the mineralogical and chemical composition of the complex crust-mantle boundary that varies in depth from 25 to 55 km.

Petrological and geochemical studies have been carried out on upper mantle and lower-crust xenoliths from Europe (e.g. Rudnick,1992; Downes,1993; Halliday *et al.*, 1993; Szabo' and Taylor, 1994; Vaselli *et al.*, 1995), North America (e.g. Best, 1975; Wilshire and Shervais, 1975; Frey and Prinz, 1978; Sen, 1988), Australia (e.g. Frey and Green, 1974; Irving, 1974; O'Reilly and Griffin,1985, 1987, 1995; Griffin and O'Reilly, 1987; O'Reilly *et al.*, 1989) and Central Asia (Stosch *et al.*, 1986, 1995; Rudnick, 1992; Kopylova *et al.*, 1995) to understand the petrological and geochemical composition of the lithosphere. Such studies are relatively rare in India, particularly from the Deccan Flood Basalt province of west central India.

The alkaline members of the coast-parallel mafic dyke-swarm intrusive into the late Cretaceous to Eocene Deccan Traps (Fig. 1) at Murud-Janjira, have entrained a variety of xenoliths including ultramafic, mafic and felsic types (Dessai, 1985) and clinopyroxene and amphibole megacrysts. Although the petrography of the xenoliths has been described elsewhere (Dessai, 1987), no account of the geochemistry of these rocks is available in the international literature. This work reports the chemistry of clinopyroxenites and phlogopite-bearing mafic granulite xenoliths from the Deccan Traps. The study also attempts to document the lithologic variation in the lithosphere beneath one of the thickest volcanic sequences of the world and evaluate the characteristics of the lower crust affected by plume-type magmatic activity (Morgan, 1981) about which little is known. Finally we discuss the nature of the deep

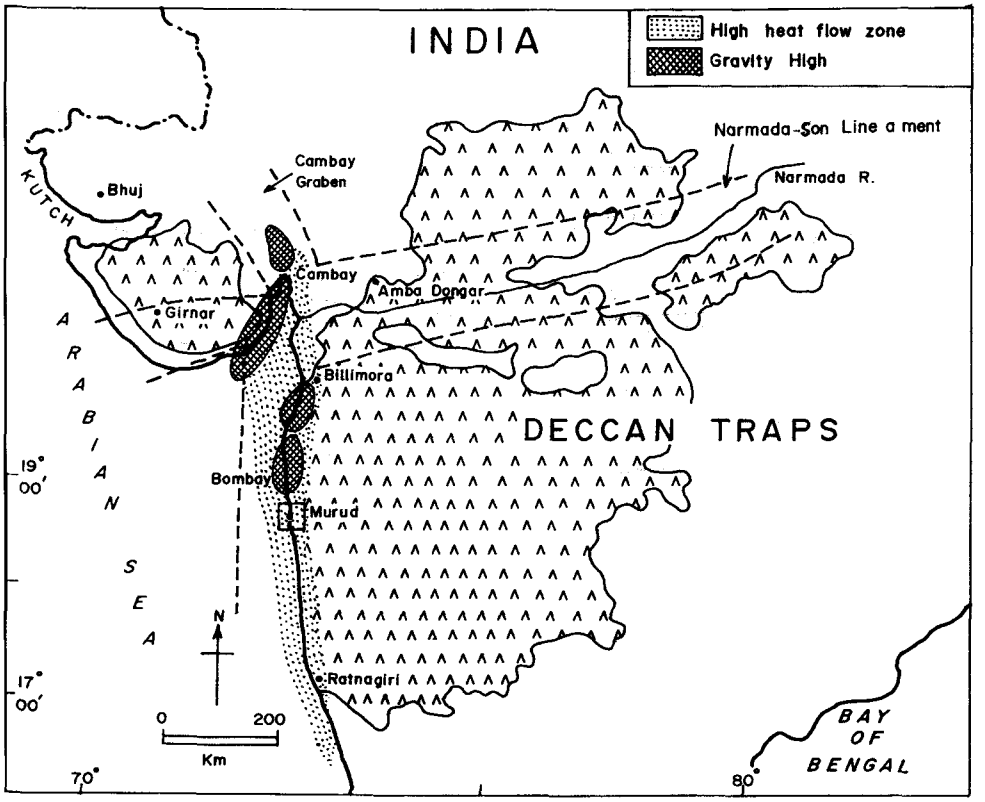

FIG. 1. Location map of the Deccan Flood Basalt province showing the xenolith site, major lineaments, gravity highs and high heat flow zone (after Mahoney, 1988; Ravi Shankar, 1988).

crust boundary by integrating the results of geochemistry with heat flow and seismic data.

Geology of the dyke-swarm

The alkaline magmatism marks the waning of the Deccan volcanic episode and immediately post-dates a period of intense tholeiitic eruptions, the lavas of which cover an area of over 0.8 million km^2 (Watts and Cox, 1989) and attain a maximum thickness of 1.7–2 km along the Western Ghat escarpment (Holmes, 1965; Kaila *et al.*, 1981). The volcanism occurred in an extensional tectonic setting with attendant lithospheric thinning and has been ascribed to the upwelling of mantle plume currently located at Reunion Island (Morgan, 1981, Cox, 1983; Richards *et al.*, 1989).

The coast-parallel mafic dyke-swarm (Auden, 1949) which straddles the continental margin 'Panvel Flexure' (Dessai and Bertrand, 1995) is intrusive into the coastal traps and is best exposed at the foot of the escarpment. The coastal traps are assigned to the Poladpur and Ambenali Formations of the Deccan Basalt Group (Subbarao and Hooper,1988) dated between 65–69 Ma (Courtillot *et al.*, 1988; Duncan and Pyle, 1988) straddling the K-T boundary. In terms of intrusive age the dykes belong to four groups (Dessai and Viegas, 1995). The early dykes are tholeiitic whereas the late ones are alkaline lamprophyres up to 2 m wide.

Petrography

Xenolith characteristics

The lithospheric xenoliths and megacrysts (>5 mm in diameter including those from fragmented and disaggregated xenoliths) are hosted by the lamprophyres (monchiquite, camptonite to

damkjernites; Dessai *et al.*, 1990). The ultramafic xenoliths are subrounded, usually ~1–2 cm in diameter and occasionally up to 5 cm. The mafic granulites and the felsic xenoliths vary in size, 2–20 cm in diameter. The xenolith population from the Deccan lamprophyres can be divided into four groups. (1) Peridotites: These are extremely rare and are represented by wehrlites (Dessai, 1985). They are usually very small (0.5–1 cm), the majority are fragmented, and they commonly occur as aggregates of a few mineral grains distributed throughout the host rock. Spinel peridotite xenoliths from Deccan are, however, reported from Kutch (Krishnamurthy *et al.*, 1988). (2) Pyroxenites: These are dominated by clinopyroxenites. A few xenoliths, however, contain trace orthopyroxenes, these are included under websterite. The former consist of clinopyroxene + opaque oxides + phlogopite + sulphides (Appendix 1). The latter are dominated by clinopyroxene + orthopyroxene (trace) + opaque oxides. Orthopyroxene occurs as exsolution blebs in clinopyroxene. Rare polygonal grains of orthopyroxene represent recrystallized exsolved material. Websterites may be gradational to the pyroxenites and appear to have evolved through aluminous pyroxenites. (3) Granulites: These consist of two-pyroxene granulites and garnet granulites. The former are made up of clinopyroxene + plagioclase + garnet + spinel + rutile and/or orthopyroxene. They invariably contain trace amounts of phlogopite. The garnet granulites consist of clinopyroxene + garnet + plagioclase. Kaersutite, apatite and sulphides vein the granulites. Some of the granulites (e.g. 281W) are composite with layers of clinopyroxenites and are also veined by the latter. (4) Granites: This group includes hypidiomorphic, granular sodic granites and felsic syenites. The latter are equigranular and are made up of K-feldspar + plagioclase + aegirine augite and opaque oxides.

Of the four groups described above, only the pyroxenites and the granulites are discussed in this paper.

The pyroxenites belong to the Al-augite group (Wilshire and Shervais, 1975) which is equivalent to the Type II xenoliths of Frey and Prinz (1978). These are considered to represent cumulates of basaltic melts, re-equilibrated and metasomatized to varying degrees.

The clinopyroxenites exhibit textures transitional between porphyroclastic (Mercier and Nicholas, 1975) and equigranular still retaining some relict porphyroclasts. The latter have serrated curvilinear outlines, strain-shadows and deformation lamellae. In some xenoliths, clinopyroxene shows exsolutions of orthopyroxene. Some samples exhibit a foliation (281X) controlled by the preferred orientation of clinopyroxene. In these textural types too, relict porphyroclasts are seen.

Secondary minerals have formed by reaction with silicate melt. Glass veins contain tiny clinopyroxene crystals which also occur in melt pockets. This clinopyroxene is here referred to as 'secondary'. Phlogopite is anhedral and intergranular (Fig. 2*a*). It occurs within clinopyroxene and is also seen to enclose it. Sulphides occur as megacrysts (>5 mm) and are represented by pyrite, chalcopyrite, pyrrhotite and pentlandite. In fragmented xenoliths, spinel has reacted with the host magma to form opaque oxides.

The mafic granulites are medium grained (2–5 mm). Samples dominated by plagioclase (281VI) exhibit equant granoblastic texture (Fig. 2*b*). Those dominated by clinopyroxene show porphyroclastic (Fig. 2*c*) and meta-igneous textures that often appear to be those of cumulates with a mild metamorphic overprint. Preferred orientation of clinopyroxene and plagioclase in some samples (281C1) may suggest original igneous layering. Pale pink garnet is altered along its borders to double rims of cryptocrystalline kelyphite in which relicts of fresh garnet are visible. The garnet contains inclusions of clinopyroxene and may be also veined by the latter (Fig. 2*d*). In some samples (e.g. 267 RHA) rutile + magnetite + plagioclase form the bulk of the rock with trace amounts of clinopyroxene.

Orthopyroxene occurs as both inclusions in clinopyroxene and as recrystallized grains. Phlogopite is anhedral and intergranular. It is found enclosing clinopyroxene and is also included in it. Spinel is anhedral in porphyroclastic types and intergranular in recrystallized xenoliths. In some xenoliths, veins of plagioclase and rarely apatite traverse clinopyroxene.

Composite xenoliths (e.g. 281W) are rare. In such xenoliths granulite contains layers of clinopyroxenite and is veined by clinopyroxene. The granulite shows equant granoblastic texture whereas the clinopyroxenite is xenomorphic granular.

Mineral chemistry

The different mineral phases from the xenoliths were analysed using a K-OS electron probe

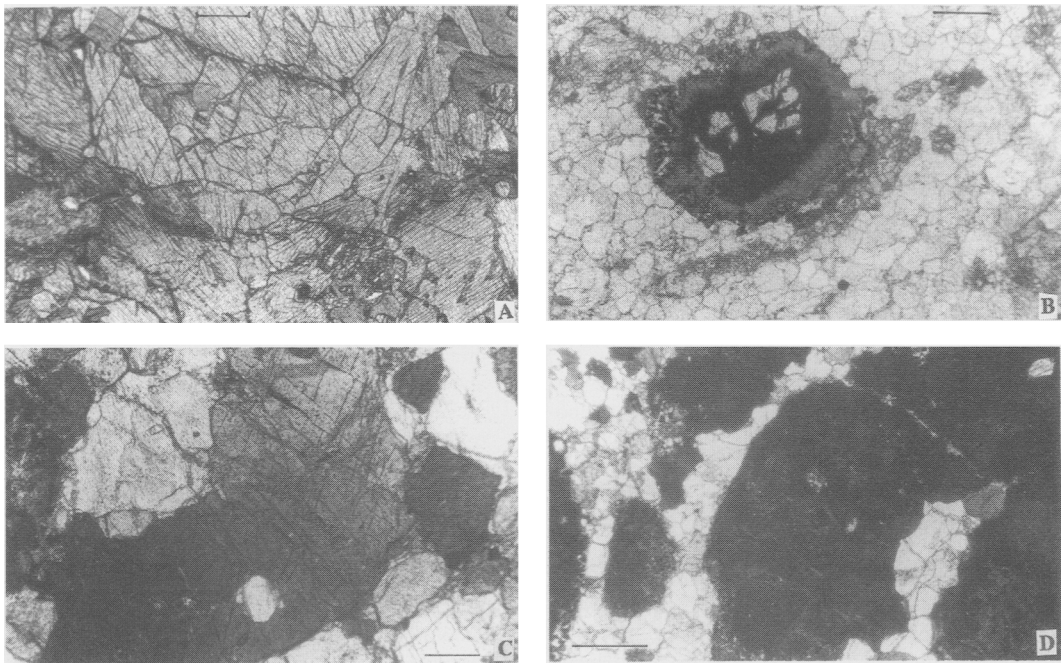

FIG. 2. (*a*) Intergranular phlogopite in clinopyroxenite xenolith, scale bar: 500 μm; (*b*) xenomorphic granular texture of plagioclase-rich granulite, scale bar: 800 μm; (*c*) deformed clinopyroxene porphyroclast with exsolution of orthopyroxene in granulite, scale bar: 500 μm; (*d*) garnet veined by clinopyroxenite in granulite, scale bar: 1000 μm.

microanalyser Super Jeol 8600 electron probe under standard operating conditions at the University of Florence (Italy). An accelerating potential of 15 kV and a specimen current of 10 nA were used. A range of natural and synthetic standards was used for comparison. Total iron was determined as FeO. Fe_2O_3 was computed on the basis of mineral stoichiometry following the method of Droop (1987). Representative analyses are presented in Tables 1–3.

Clinopyroxenes from the pyroxenites have compositions essentially within the En-Di-Hd-Fs quadrilateral, with the majority being ferroan diopsides [*sensu* Morimoto *et al.*, 1988; Ca_{43-49} Mg_{43-49} Fe_{07-11} $Mg\#(Mg/(Mg+Fe^{+2}))$ 0.83–0.95]. Some, however, are sodian diopsides and Mg-rich augites (281VII). The aegirine component in them is 5–11 mol.% in the rims. MgO in general is >14 wt.%, TiO_2 >7 wt.% and Al^{VI} <0.03 wt.%. Clinopyroxenes from the granulite xenoliths are sodian ferroan diopsides and aluminian ferroan diopsides (Morimoto *et al.*, 1988; Ca_{46-56} Mg_{33-43} Fe_{9-13}, Mg# = 0.82–0.92). Compared with the pyroxenite clinopyroxenes, these have lower MgO (<14 wt.%) and TiO_2 (<0.4 wt.%) and higher Al^{VI} (with the jadeite component varying between 2–8 mol.%). They are also more calcic (Ca# = 0.54-0.62, i.e. (Ca/Ca+Mg)) than those from pyroxenites (Ca# = 0.48–0.55).

Clinopyroxenes from the pyroxenites and granulites can be distinguished in major element variation diagrams (Figs 3, 4). Titanium and Al show negative correlation indicating that Ti preferentially substitutes for Al in the pyroxene lattice in the octahedral site to compensate for Al^{3+}-Si^{4+} substitution. The Ti and Al^{IV}, show no correlation, however. The granulite clinopyroxenes have a higher content of Al^{VI} and a lower Ti/Al ratio than those from the clinopyroxenites. The former could be interpreted as an effect of interaction with the melt as is evident from the composition of the clinopyroxene in melt pool (Table 1, analysis 23). In an Ac-(Di+CaTs)-Jd plot (Fig. 5), the clinopyroxenes plot within the overlapping Group A and B fields for eclogites (Mottana, 1986). The clinopyroxene in clinopyroxenite layers in composite granulite xenoliths

TABLE 1. Electron probe microanalyses of pyroxenes in xenoliths from Murud-Janjira

	Sample	SiO_2	TiO_2	Al_2O_3	Cr_2O_3	FeO	MnO	MgO	CaO	Na_2O	Total
1	281X	51.80	0.80	1.93	0.00	6.12	0.11	14.32	23.96	0.80	99,84
2	281X	52.55	0.68	1.35	0.00	6.15	0.20	14.04	23.33	0.84	99.14
3	281X	51.54	0.87	2.03	0.02	6.64	0.11	13.82	23.55	0.95	99.53
4	281X	52.83	0.81	1.28	0.00	5.55	0.16	14.65	24.07	0.72	100.07
5	281X	51.01	1.12	2.72	0.03	5.36	0.11	14.55	24.00	0.60	99.50
6	281X	52.44	0.91	2.04	0.00	7.01	0.18	13.64	23.28	0.97	100.47
7	281VII	52.44	0.87	2.12	0.20	6.39	0.11	15.50	20.99	1.01	99.63
8	281VII	52.55	0.68	2.05	0.27	6.53	0.14	14.73	21.52	1.33	99.80
9	281VII	52.32	0.73	1.95	0.23	6.27	0.08	15.03	21.65	1.21	99.47
10	281VII	52.91	0.54	1.95	0.16	6.08	0.12	14.81	21.43	1.25	99.25
11	281W	52.19	0.34	4.43	0.13	6.47	0.05	13.39	21.04	1.70	99.74
12	281W	52.43	0.40	4.40	0.14	6.72	0.07	13.11	20.78	1.60	99.65
13	281W	51.67	0.44	4.71	0.12	6.93	0.03	13.28	21.13	1.61	99.92
14	281W	52.98	0.39	3.81	0.14	6.38	0.01	14.04	21.38	1.36	100.49
15	281VI	51.51	0.34	4.82	0.02	7.12	0.06	12.31	21.68	1.75	99.61
16	281VI	47.39	1.01	8.01	0.00	8.10	0.06	12.50	22.24	0.67	99.98
17	281VI	51.79	0.30	4.23	0.04	6.97	0.03	12.77	21.60	1.76	99.49
18	281VI	52.38	0.35	4.75	0.12	6.94	0.00	12.50	21.29	1.75	100.08
19	281W	52.78	0.33	3.81	0.14	5.47	0.06	14.21	21.73	1.48	100.01
20	281W	52.29	0.54	4.19	0.12	6.63	0.06	13.71	21.31	1.46	100.31
21	281D	51.88	0.30	3.09	0.09	9.95	0.07	12.41	21.41	1.11	100.31
22	281B	41.80	2.99	12.05	0.10	12.95	1.39	6.47	21.82	0.85	100.42
23	281C	49.96	0.17	9.54	0.03	7.22	0.56	15.59	17.20	0.69	100.96
24	281C	53.25	0.02	7.29	0.03	9.91	0.65	27.80	1.85	0.00	100.80
25	281W	47.28	0.26	8.64	0.07	23.68	0.62	17.94	1.78	0.00	100.27
26	281W	54.20	0.04	1.29	0.04	18.86	0.20	25.81	0.54	0.00	100.98

1–10: cpx porphyroclast, cpxinite; 11–18: cpx porphyroclats, granulite; 19: vein cpx, granulite; 20: cpx inclusion in garnet, granulite; 21–22: 'secondary' cpx, cpxinite; 23: cpx in melt pool, cpxinite; 24: opx in melt pool, cpxinite; 25: opx in garnet vein, granulite; 26: opx adjacent to plag., granulite

TABLE 2. Electron probe microanalyses of minerals in xenoliths from Murud-Janjira

	Garnets							Plagioclases					
	1	2	3	4	5	6	7	8	9	10	11	12	13
wt%/Smp	281W	281W	281VI	281VI	281W	281W	281W	281W	281W	281VI	281VI	281VI	281VI
SiO_2	40.01	40.14	39.45	39.44	40.30	39.88	39.97	60.65	61.26	59.35	60.52	60.38	60.45
TiO_2	0.03	0.03	0.07	0.08	0.04	0.02	2.42	0.00	0.04	0.04	0.00	0.00	0.00
Al_2O_3	21.98	24.30	21.80	21.58	21.90	21.86	21.56	25.12	24.35	25.60	25.28	25.55	25.24
Cr_2O_3	0.13	0.16	0.05	0.11	0.16	0.14	0.10	0.00	0.01	0.03	0.00	0.00	0.00
FeO	21.90	18.86	23.61	23.40	22.10	22.60	21.79	0.09	0.12	0.10	0.23	0.07	0.07
MnO	0.51	0.48	0.51	0.56	0.48	0.59	0.48	0.01	0.03	0.00	0.04	0.02	0.00
MgO	10.51	9.25	8.31	8.03	10.30	10.12	10.75	0.04	0.00	0.00	0.05	0.00	0.03
CaO	5.54	7.09	7.22	7.20	5.41	5.60	5.53	6.24	5.686,84		6.69	6.74	6.09
Na_2O	0.00	0.00	0.12	0.04	0.00	0.00	0.00	7.89	8.53	7.57	7.65	7.84	7.94
K_2O	–	–	–	–	–	–	–	0.30	0.36	0.36	0.41	0.35	0.48
Total	100.61	100.31	101.14	100.44	100.69	100.81	101.70	100.34	100.38	99.89	100.87	100.95	100.30

TABLE 3. Electron probe microanalyses of minerals in xenoliths from Murud-Janjira

	Spinels								Phlogopites				
	1	2	3	4	5	6	7	8	9	10	11	12	13
wt%/Smp	281X	281X	281X	281X	281W	281W	281W	281C	281VII	281VII	281VII	281E	281E
SiO_2	0.04	0.05	0.01	0.02	0.08	0.07	0.03	0.18	40.29	40.80	40.47	40.17	38.38
TiO_2	11.59	12.60	11.58	13.01	0.57	0.16	49.84	0.13	3.80	3.88	3.70	4.48	6.23
Al_2O_3	1.33	0.87	1.18	0.39	54.82	58.52	0.66	65.64	15.07	14.71	14.55	14.38	14.52
Cr_2O_3	0.04	0.03	0.04	0.02	0.77	1.02	0.18	0.21	0.26	0.27	0.21	0.73	0.02
FeO	83.55	82.27	83.16	81.81	33.83	23.52	44.12	13.21	10.08	9.54	10.24	8.78	12.09
MnO	0.89	0.88	0.86	0.92	0.34	0.14	0.37	0.25	0.09	0.06	0.04	0.00	0.12
MgO	2.54	3.27	3.13	3.72	9.70	15.57	4.77	20.35	20.34	20.17	20.48	20.48	17.31
CaO	–	–	–	–	–	–	–	–	0.04	0.24	0.06	0.00	0.04
Na_2O	–	–	–	–	–	–	–	–	1.16	1.17	1.12	0.88	1.34
K2O	–	–	–	–	–	–	–	–	8.80	9.02	9.09	9.28	8.06
F	–	–	–	–	–	–	–	–	0.00	0.00	0.00	0.78	1.56
Total	99.98	99.97	99.96	99.89	100.16	99.00	99.97	99.97	99.93	99.86	99.96	99.96	99.67

(e.g. 281W) is compositionally similar to clinopyroxene porphyroclasts in the clinopyroxenites.

Orthopyroxene is rare but may occur in some xenoliths either as discrete grains, exsolutions in clinopyroxene and/or inclusions within garnet veins. Compositionally the orthopyroxenes are aluminian ferroan enstatites (Morimoto *et al.*, 1988). Orthopyroxenes included within garnet have Mg# = 0.59, whereas those in contact with plagioclase have Mg# 0.72 (Table 1, analyses 25 and 26 respectively). More magnesian orthopyroxene (Mg# 0.83) also occurs in melt pockets in the clinopyroxenites (Table 2, analysis 24). It can be classified as aluminian ferroan enstatite ($Ca_4Mg_{79}Fe_{17}$; Mg# = 0.83, Ca# 0.04; $Al^{VI} = 0.16$).

Garnets are rich in almandine (45–49%). The pyrope (30 39%), and grossular (14- 19%) components show considerable variation unrelated to the modal composition. Most of the garnets do not exhibit significant zoning (Table 2). They show compositional similarity to garnets in 'igneous' eclogites and to garnets in garnet-clinopyroxene-plagioclase-bearing xenoliths in diatremes, which, according to Mottana (1986) are also granulites by definition. Garnet rims are invariably altered to kelyphite (Table 2, analyses 6 and 7) which show slight variation in composition from unaltered garnet core.

Plagioclase is the only feldspar phase present. It shows very limited compositional variation within a sample ($An_{29-36}Ab_{68-63}Or_{3-1}$; 281VI) but slightly larger variation between samples. The majority of analysed grains show no appreciable zoning (Table 2).

Spinels from the pyroxenites belong to the magnetite series and form a solid solution between ulvospinel and magnetite. The grains are slightly zoned. Fe-spinel (*sensu stricto*) and ilmenite occur in granulite (281W). Spinel (*sensu stricto*) occurs in melt-pockets in reacted xenoliths (281C). It is aluminous (Al_2O_3 = 64.65 wt.%, Mg# = 0.76, Cr# = 0.21) in nature (Table 3, analysis 8). Phlogopite in the pyroxenites (Mg# 0.76–0.79) has an Mg/Fe ratio varying between 3.3 3.7. Those in contact with kelyphite have a very low Mg# (0.11–0.27) and their Mg/Fe ratio varies from 0.16–0.38. Phlogopite in reacted xenoliths contains 0.77 wt.% F in the core increasing to 1.52 wt.% in the rim (Table 3, analyses 12 and 13). The phlogopite shows similarities with type II micas, and more specifically to type-B micas, from Jos calcite kimberlite (Mitchell, 1986). Considering their high Al_2O_3 (>14 wt.%) and high TiO_2 (>4 wt.%) the micas are primitive.

P-T conditions

Equilibration temperatures were estimated from major element compositions of minerals using the two-pyroxene thermometers of Wells (1977), and Wood and Banno (1973) and the single pyroxene thermometer of Mercier (1980). The pressures were calculated using geobarometric calibrations of Newton and Perkins (1982), Powell and

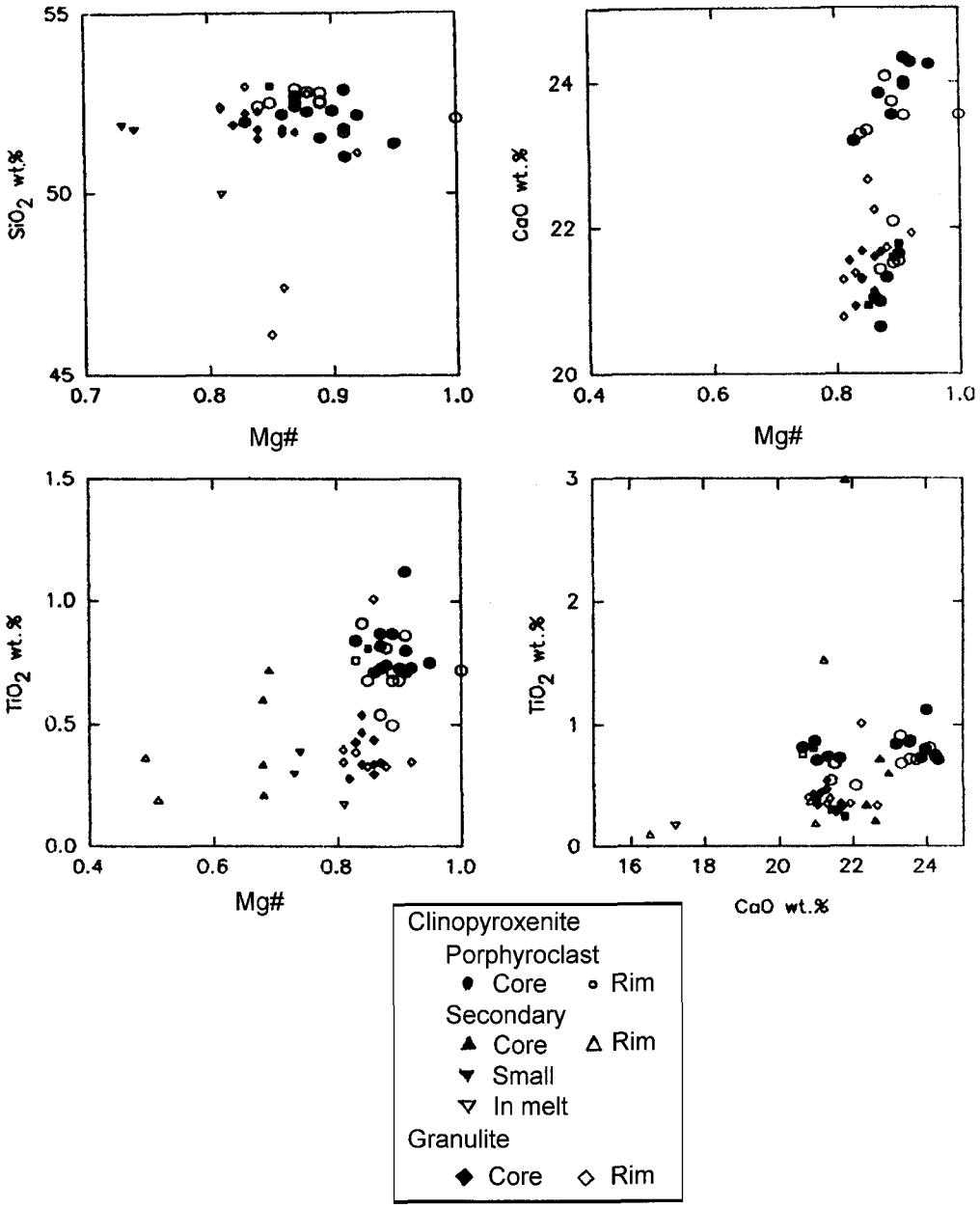

FIGS. 3,4. Major element variations in clinopyroxenes for xenoliths from Murud-Janjira.

Holland (1988) and Mercier (1980). Although zoning in minerals is insignificant, only core compositions were considered when calculating the *P-T* estimates, as a precaution.

Because it was impossible to determine Fe^{3+} in the microprobe analysis, there are considerable limitations in the calculation of *P-T* conditions. One way to overcome this difficulty is to apply

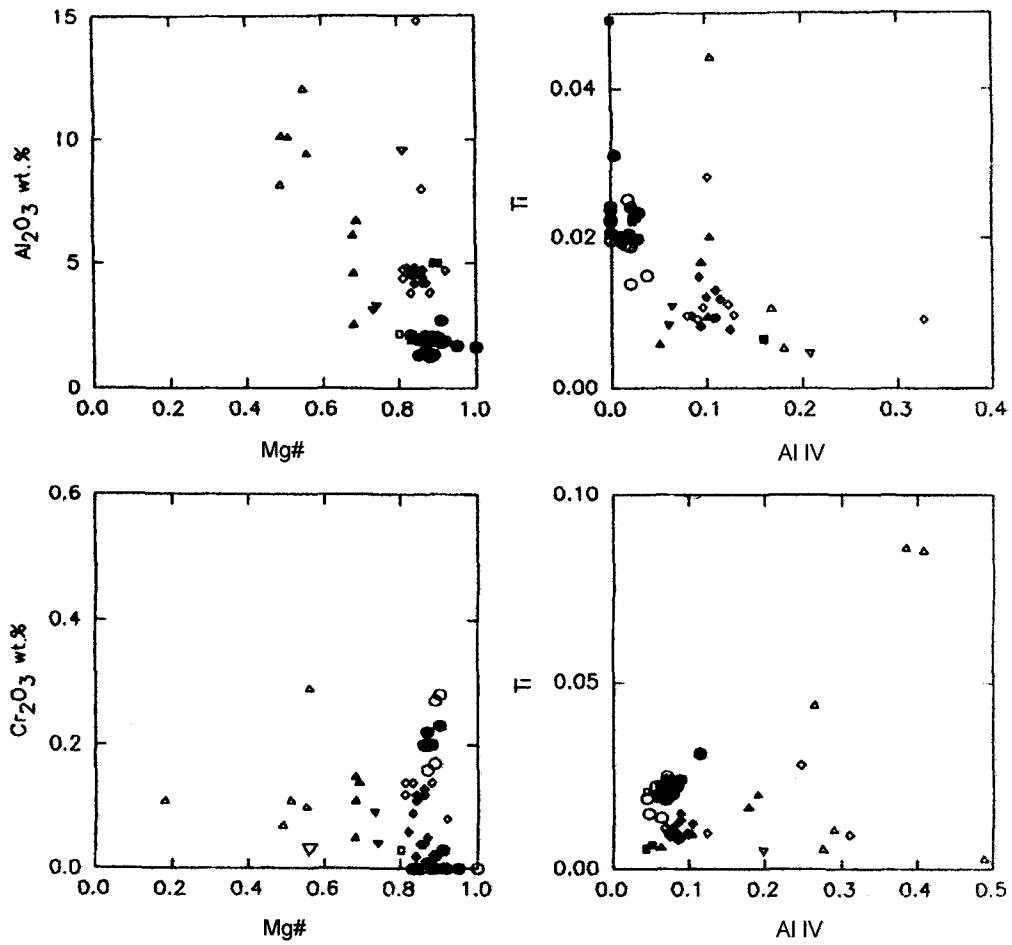

FIG. 4.

the Wood and Banno (1973) and Wells (1977) geothermometers as these methods do not rely on Fe^{2+} and Fe^{3+} content or on the presence of other minerals in the assemblage.

The temperatures estimated (Table 4) by two of these methods are consistent and indicate equilibration at ~825–870°C for the granulite xenoliths. A reference pressure of 15 kbar was used in temperature computations. A fragmented clinopyroxenite shows a temperature of >1100°C. If the temperatures shown by the fragmented clinopyroxenite xenolith minerals (those in melt pockets) are taken as ambient, then it could be inferred that clinopyroxenites formed at higher temperatures than the granulites and subsequently re-equilibrated. Broadly speaking, the temperature range for the pyroxenite xenoliths is similar to those from Massif Central in France (Brown *et al.*, 1980) and eastern Transylvania (Vaselli *et al.*, 1995); however, the estimates are based on a disequilibrium assemblage and hence caution needs to be exercised. The pressures estimated by two of the above calibrations show values between 11 and 14 kbar. Powell and Holland (1988) calibration gives values 2 kbar greater than those done by the Newton and Perkins (1982) calibration.

Whole rock geochemistry

Four representative clinopyroxenite xenoliths (>3 cm in diameter) and the host rock were analysed for major, trace and rare earth elements

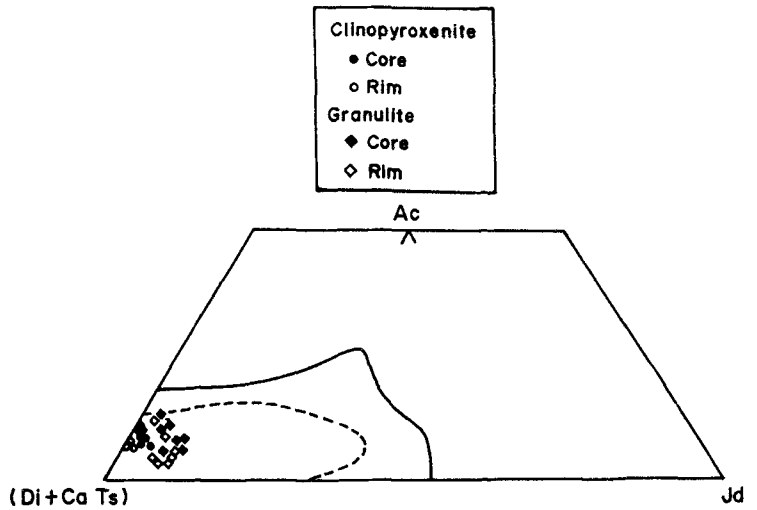

FIG. 5. Clinopyroxene compositions in Ac-(Di+Ts)-Jd plot (solid line: field of Group B eclogites; dashes: field of Group A 'igneous' eclogites; after Mottana, 1986).

at the National Geophysical Research Institute (NGRI) at Hyderabad. The major elements were analysed by X-ray fluorescence spectrometry. The trace and rare earth elements (*REE*) were determined by inductively coupled plasma spectrometry (ICP-MS). The Fe_2O_3 was calculated from total iron (as FeO) following Le Maitre (1976). Analytical precision and accuracy were controlled by replicate analysis of international reference standards.

Whole rock concentrations of major and trace elements are presented in Table 5 (Dessai, 1996). All clinopyroxenites are ultrabasic including 281P and 281Q (SiO_2 >45%, TiO_2 >3 wt.%, Mg# >0.85) which, although they have >45% SiO_2, also contain >15.8% MgO and hence could be categorized as ultrabasic. All samples are nepheline-(281P and Q) and leucite-(281R and S) normative. The Mg# shows an inverse relationship with SiO_2, Al_2O_3, FeO, Na_2O and total alkalis. This relationship is similar to the trends observed in ultrabasic xenoliths world wide (e.g. Kuno and Aoki, 1970; Frey and Prinz, 1978). Their high Mg# and low Al_2O_3 content (<8 wt.%) suggests that some have originated as cumulates of relatively primitive mantle melts. The total alkalis are lower in samples with low Al content. These levels are consistent with crystallization and accumulation of clinopyroxene from the parent melt.

The pyroxenites 281P and 281Q have lower K_2O, TiO_2, Al_2O_3 and FeO contents than 281R and 281S. Low K_2O and TiO_2 are consistent with modal mineralogy dominated by clinopyroxenes. The xenoliths show a negative correlation between normative feldspar + nepheline and

TABLE 4. *P-T* estimates of xenoliths from Murud-Janjira

Rock Type	Wood & Banno (1973) *T*°C	Wells (1977) *T*°C	Newton & Perkins (1982) *P* (kbar)	Powell & Holland (1988) *P* (kbar)	Mercier (1980) *T*°C	Mercier (1980) *P* (kbar)
Clinopyroxenite	910	846			832–1256	11–13
Granulite (281W)	810–840	820–870	11	13.5	870–920	15–20
Disagg. clinopyroxenite	1154	1110			1256	23

TABLE 5. Whole rock major (oxide wt.%) and trace element (ppm) analyses of xenoliths and host rock from Murud-Janjira

Sample No. Constituents	281	281P	281Q	281R	281S	281VI	281W
SiO_2	44.35	48.18	49.30	43.63	42.17	51.73	49.24
TiO_2	3.47	0.22	0.23	3.92	3.69	1.39	2.26
Al_2O_3	12.58	5.45	5.58	6.50	8.29	15.13	12.88
Cr_2O_3	0.25	0.92	0.66	0.15	0.20	0.03	0.12
Fe_2O_3	6.12	3.23	3.30	4.98	4.82	n.d.	n.d.
FeO	8.73	4.61	4.71	7.11	6.88	7.44	11.93
MnO	0.18	0.07	0.07	0.16	0.16	0.22	0.21
MgO	9.35	17.50	15.86	15.84	15.31	8.27	8.85
CaO	9.14	17.95	18.37	15.39	16.48	11.94	12.20
Na_2O	3.71	1.21	1.23	1.71	1.66	3.40	2.22
K_2O	1.52	0.22	0.22	0.88	0.86	0.29	0.25
P_2O_5	0.54	0.40	0.42	0.08	0.08	0.14	0.10
Total	99.94	99.96	99.95	100.35	100.60	99.98	100.00
Trace Elements							
Sc	23.24	15.80			49.03	n.d.	
V	209.68	161.66			274.33	53.00	
Cr	447.16	8193.86			1801.99	125.00	
Co	60.82	26.78			74.34	27.20	
Ni	269.40	200.14			574.41	146.00	
Cu	232.06	655.57			806.11	37.00	
Zn	202.97	153.14			166.89	28.00	
Ga	16.61	10.35			10.22	15.00	
Rb	46.31	2.68			11.06	13.70	
Sr	1728.97	225.59			449.54	503.88	
Y	24.01	9.11			12.60	3.40	
Zr	378.43	35.03			122.49	48.00	
Nb	131.95	1.41			35.51	22.40	
Cs	0.63	0.07			0.62	0.20	
Ba	1080.25	104.56			181.29	825.50	
Hf	8.72	1.25			4.00	0.90	
Ta	9.08	0.11			2.67	1.15	
Pb	15.68	22.83			11.83	n.d.	
Th	18.96	0.69			1.58	1.84	
U	4.37	1.12			0.44	0.41	
La	177.39	22.93			25.61	16.23	
Ce	316.77	32.88			57.85	29.02	
Pr	34.70	4.12			7.81	2.41	
Nd	119.90	15.24			31.10	9.39	
Sm	14.87	2.72			4.95	1.55	
Eu	4.10	0.81			1.58	0.79	
Gd	12.00	2.67			4.18	1.14	
Tb	1.37	0.35			0.64	0.16	
Dy	6.05	1.66			2.87	0.71	
Ho	0.79	0.27			0.46	0.13	
Er	1.98	0.70			1.06	0.36	
Tm	0.26	0.10			0.15	0.04	
Yb	1.79	0.41			0.89	0.32	
Lu	0.24	0.08			0.16	0.04	

281: monchiquite; 281P and Q: garnet clinopyroxenite; 281R and S: clinopyroxenite; 281VI and 281W: granulites. n.d.: not determined

normative pyroxene + olivine and show compositional similarity to the granulite facies plagioclase-free rocks from Lesotho (Griffin *et al.*, 1979).

The granulites are basic (SiO_2: 49.2–51.7 wt.%), MgO varies between 8.2 and 8.8 wt.%. Na_2O is higher in samples dominated by plagioclase (281VI) than those (281W) in which plagioclase is present in a lower concentration. The former contains less MgO than the latter and yet has a higher Mg# (0.66 as opposed to 0.56), because of higher modal abundance of Fe-oxides in the latter sample. Both rocks are olivine normative.

Compatible trace elements such as Cr and Ni show high concentrations, large variation between samples and exhibit a positive correlation with Mg#, whereas the incompatible elements such as Rb, Y, Zr, Nb, Sc, Hf and the rare earth elements (*REE*) show negative correlations. Broader variation of compatible elements has been attributed to cumulate crystallization (Frey and Prinz, 1978). In terms of incompatible element ratios, 281P has a Rb/Nb ratio of 1.9 which is close to the average Indian basic amphibolite (Rb/Nb = 1.8; Peng *et al.*, 1994), whereas the Rb/Nb ratio (0.31) of 281S lies between the values of oceanic and continental mantle derived rocks (e.g. Peng *et al.*, 1994). The Th/Yb (1.68) and Ta/Yb (3.0) ratios of the latter are similar to enriched mantle.

Incompatible element concentrations are low in granulites. Although it is not advisable to make generalizations on the basis of one analysis, some tentative statements can be made on the geochemical features. The Th/U ratio of ~4 is typical of granulite (Taylor and McLennan, 1985). The Sm/Nd ratio (0.16) is closer to an upper crustal value (0.17) but Rb/Sr (0.027) is much lower compared with the upper crustal value of 0.3 (Taylor and McLennan, 1985). The Rb/Nb ratio (0.6) is similar to E-MORB.

In a primitive mantle-normalized LIL element 'spider diagram' (Fig. 6), the patterns of the host rock (281) and the xenolith (281S) are closely similar. This is probably the effect of equilibration of the xenolith with the host. As regards 281P, the 'spiderdiagram' shows pronounced troughs at Nb-Ta, Zr and Ti which reflect the modal composition of the xenolith. These high-field strength elements (HFSE) reside largely in the opaque oxides which are rare in the xenolith. The peaks at Nb-Ta and Ti in 281S could be attributed to equilibration with the alkaline host. The troughs at Nb, Ta, Zr and Ti could be ascribed to modal mineralogy and to residual phlogopite in the mantle source (Wilson, 1989) or

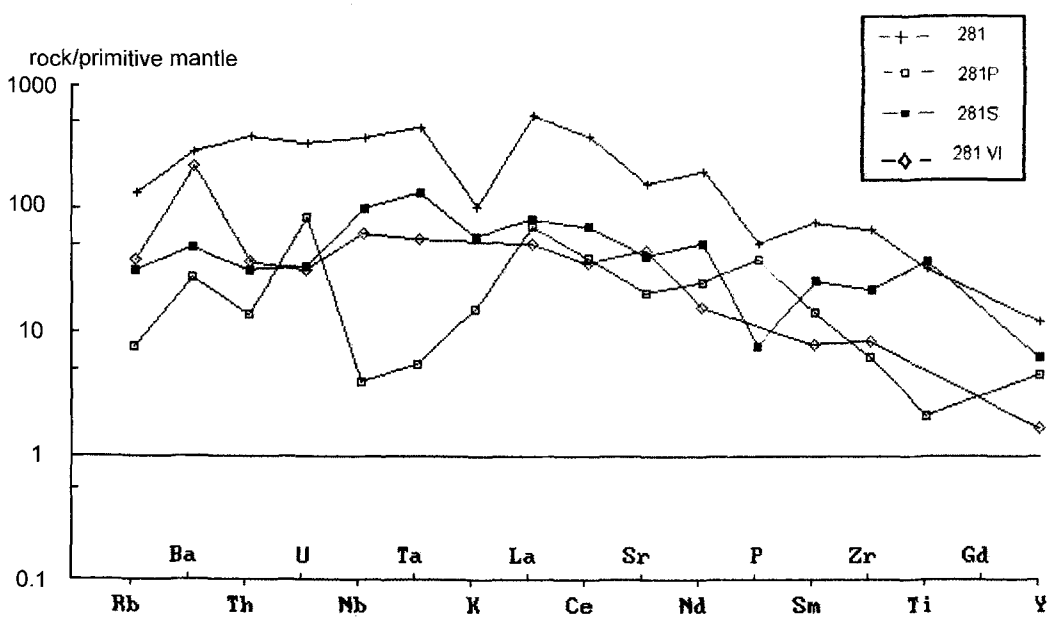

FIG. 6. Mantle normalized spider diagram of clinopyroxenite xenoliths from Murud-Janjira (normalization after Sun and McDonough, 1989).

to crustal contamination (e.g. Cox and Hawkesworth, 1985) which seems unlikely in the case of xenoliths. The 'spider diagram' of the granulite (281VI) shows a peak at Ba and troughs at Th and U. The pattern is consistent with that of a mafic granulite xenolith from Lesotho (Taylor and McLennan, 1985). Rubidium shows depletion relative to Sr as is also observed in some south Indian granulites (e.g. Taylor and McLennan, 1985).

The *REE* patterns of the xenoliths and the host are presented in Fig. 7. The patterns of the clinopyroxenite xenoliths are strongly *LREE* enriched, and similar to that of the host (281). The La abundance ranges from 15–70 times the chondritic value. The Yb content is, however, very low and is only 2–4 times chondrite. In fact the concentration of heavy *REE* in 281P should have been higher as expected from modal mineralogy, but instead the Ce/Yb ratio of 281P is greater (16) than that of 281S. Smooth variation of *REE* patterns particularly that of 281P suggests metasomatic overprint. The other two patterns (281 and 281S) may be related to closed system crystallization and equilibrium of 281S with the host melt. The pattern of the granulite xenolith (281VI) shows a distinct positive Eu anomaly. The heavy *REE*s do not show any effect despite the presence of garnet. This could be taken to indicate that bulk rock Eu enrichment had taken place prior to the crystallization of garnet in the granulite facies of metamorphism (e.g. Taylor and McLennan, 1985).

Discussion

Nature of continental lithosphere

The mineralogical and the geochemical characteristics of the xenoliths indicate that the lithospheric column sampled by the lamprophyres is dominated by clinopyroxenites. This suggests that the deep crust in this region contains a system of clinopyroxenite layers. These lithologies have been subjected to mild ductile deformation as evidenced by the textural features such as porphyroclastic/equigranular transitional textures. This deformational episode could be related to extensional thinning and attenuation of the lithosphere. This may have occurred prior to the opening of the Arabian Sea (~64 Ma: Hooper, 1990; Dewey and Stephens, 1992). Fracturing of the constituent minerals and veining, marked a brittle deformational event that followed. Deformation largely preceded metamorphism but did continue afterwards to a lesser extent. Low equilibration temperatures may indicate a recrystallization event. These textural features suggest that the lower crust had witnessed deformation and metamorphism prior to the Deccan magmatism and opening of the Arabian

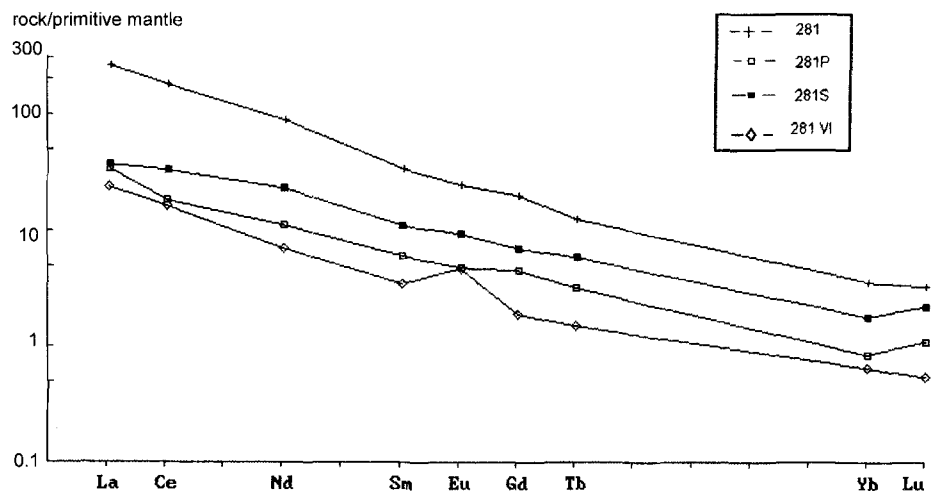

FIG. 7. Mantle normalized *REE* pattern of clinopyroxenite xenoliths from Murud-Janjira (normalization after Sun and McDonough, 1989).

Sea at ~64 Ma (Hooper, 1990; Dewey and Stephens, 1992). In peninsular India a regional tectonothermal event at ~550 Ma is well recognized (Crawford, 1969; Balasundaram and Balasubramanyan, 1973; Hanson *et al.*, 1985). On the basis of isotope data, it has been suggested recently that the last granulite facies metamorphism affected the lower crust at ~550 Ma (Choudhary *et al.*, 1992; Santosh *et al.*, 1992; Brandon and Meen, 1995). It could be inferred therefore, that some of the xenoliths at least could be related to the Pan-African tectonometamorphic event though some could be even older. As the xenolith-bearing dykes come from a region of thermal updoming in the vicinity of Bombay, it is reasonable to conclude that the xenoliths represent fragments of lithosphere torn apart and incorporated in Deccan magmas.

Metasomatic modifications

The intragrain compositional variation exhibited by the clinopyroxenes in the disaggregated xenoliths is significant. The majority of clinopyroxenes have resorbed rims indicating reaction with an infiltrated melt. The latter could be: (a) trapped host liquid; (b) a partial melt formed by decompression during ascent of the xenoliths; or (c) a trapped melt which represents the liquid remaining after the crystallization of pyroxenes. Such a liquid is particularly significant, being responsible for the formation of phlogopite. The clinopyroxenes are primary crystals whereas on textural grounds the phlogopites are regarded as secondary. The Mg# of clinopyroxenes and phlogopite are unrelated, suggesting disequilibrium. The phlogopite in the xenoliths differs from that in the lamprophyre host in having a higher Mg# and a greater Mg/Fe ratio. We conclude that xenolith phlogopite crystallized from an infiltrated magma which brought about compositional variation in the recrystallized clinopyroxenes. This could be viewed as a case of patent metasomatism (Harte, 1983).

The LIL-enriched patterns of the Murud-Janjira xenoliths although similar to that of the host lamprophyre, cannot be attributed to equilibrium with the host magma alone because if it had been so the patterns of both 281P and 281S should have been identical to the host, and such is not the case. Sample 281P is dominated by clinopyroxene which hosts the LIL elements. Additionally, the presence of garnet (16 wt.%) and trace phlogopite should have concentrated HFSE and heavy *REE*. Instead these occur in lower concentrations in 281P than in 281S. High concentration of compatible elements, several times more than the host, and their positive correlation with Mg# support a cumulative origin. The clinopyroxenites formed from a magma compositionally similar to the host but of a much older magmatic cycle. This conclusion seems to agree with similar observations in other parts of the world, e.g. Witt-Eickschen *et al.* (1993) and Vaselli *et al.* (1995) who also consider the anhydrous pyroxenites from Eifel and eastern Transylvania to be the products of an earlier magmatic episode. Alkaline magmatism in peninsular India had a protracted time span from late Proterozoic to early Palaeozoic, coinciding broadly with the Pan-African events in other parts of the Gondwanaland (Kroner, 1981).

The *LREE*-enrichment exhibited by the Murud-Janjira xenoliths is probably related to metasomatic modifications of the lithosphere. This process is related to the formation of phlogopite (e.g. Mahoney *et al.*, 1985) during which LIL element enrichment could occur. However, it need not bring about *REE*-enrichment. Moreover 281P which contains trace phlogopite is more enriched in light *REE* than 281S. The presence of garnet in the former actually should have favoured concentration of heavy *REE* which in fact is less than in 281S. Hence, though LIL enrichment may have accompanied phlogopite formation, *REE*-enrichement by cryptic metasomatism has also affected the lithosphere (e.g. Dessai *et al.*, 1990; Dessai, 1994) and this may be an independent event.

The LILE-enrichment was brought about by metasomatizing fluids possibly as a precursor to the generation of the alkaline magma (Menzies and Murthy, 1980) from which the Al-augite group of clinopyroxenes crystallized. This is in agreement with several studies based on minor element and isotope data from other parts of the world (e.g. Basu, 1978; Boettcher and O'Neil, 1980; Irving, 1980), which emphasize that the hydrous phases in the xenoliths are neither related to nor compositionally equivalent to the host basalts. It can be surmised therefore, that the mantle beneath the Deccan Traps underwent pervasive metasomatism prior to the generation of alkaline magmas. This metasomatized mantle is more favourable for the generation of alkaline magmas (Edgar, 1987). This is supported by the Nb peak in the LIL spidergram as well as by the Nb/La ratio >1 (281S) which is characteristic of rocks derived from incompatible-element

enriched oceanic mantle (Sun, 1980). Similarly, the Rb/Nb (0.31) and Ba/Nb (5.1) ratios are within the range of oceanic or continental mantle-derived rocks (Taylor and McLennan, 1985; Peng *et al.*, 1994).

Origin of Murud-Janjira xenoliths

The textural characteristics, the mineralogy dominated by mafic compositions, and the complete absence of aluminous silicates indicate that the granulite protoliths were igneous in origin. Modal and normative mineralogy (IUGS, 1973) allow classification of the magmatic protoliths as gabbros. The mineralogy of the xenolith is consistent with crystallization from melts with primitive characteristics. The presence of orthopyroxene suggests that the parental melts were sub-alkaline. The granulite xenoliths possess a limited mineralogy dominated by clinopyroxene, garnet and plagioclase with accessory orthopyroxene, rutile and mica indicative of high pressure (~11 kbar) granulite facies rocks with eclogitic affinities (Rogers, 1977).

Textural characteristics and the chemical composition of the clinopyroxenites are akin to cumulates which have probably been subjected to metasomatic modifications. They have crystallized from alkaline melts which were more primitive than those of the granulite protoliths. The pyroxenites belong to a magmatic episode that long predates the host lamprophyres. They represent segregations of mantle-derived magmas (e.g. Irving, 1980) and are therefore not cognate with their host. Textural inter-relationship between the granulites and the clinopyroxenites also suggests that the less metamorphosed and mildly deformed clinopyroxenites intra-plated the lower crust (granulite protoliths) towards the end of metamorphism, which itself could be viewed to be the result of magmatic under- and intra-plating. Lack of progressive variation in mineral composition from clinopyroxenites to granulites indicates that the Murud-Janjira suite represents a series of cumulates which crystallized from compositionally unrelated melts.

Granulite metamorphism and alkaline magmatism in peninsular India have been suggested to be closely related in time (Choudhary *et al.*, 1992; Harris and Santosh, 1993). Both the granulites as well as the clinopyroxenites have been affected by a modal metasomatic event during which phlogopite was introduced and LIL-enrichment occurred. It may be concluded therefore that the lower crust beneath Murud-Janjira was pervasively metasomatized much before the Deccan magmatism.

Structure of the deep continental crust

The mineralogy of the xenoliths is consistent with their entrainment from the continental lower crust which is widely recognized to consist of granulite facies rocks. (e.g. Griffin *et al.*, 1979; Rudnick, 1992; Stosch *et al.*, 1995; Kempton *et al.*, 1995, 1997). However, the determination of the precise composition of the deep crust is beset with difficulties. The characteristics of the xenoliths provide clues to the composition and structure of the lower crust beneath Murud-Janjira. Precise assessment of the *P-T* conditions under which the xenoliths equilibrated is difficult because of their small size, the disaggregated nature and an insufficient number of composite xenoliths. A broad *P-T* range is therefore presented, which requires refinement by additional data. The temperature range for the granulites varies from 825–870°C using the Wells (1973) and Wood and Banno (1973) geothermometers at pressures from 11–14 kbar (by the Newton and Perkins (1982) and the Powell and Holland (1988) geobarometers). Temperatures of >1100°C are indicated for the clinopyroxenites at depths of ~30–39 km. The spinel-pyroxenite–garnet-pyroxenite transition occurs at 10–12 kbar for a temperature range of 825–1025°C. The temperature estimates (825–870°C) of the Murud-Janjira granulite xenoliths correspond to the lower limit of the range (833–949°C) for spinel peridotite xenoliths from Kutch (Krishnamurthy *et al.*, 1988) using th same geothermometric methods (e.g. Wells 1977; Wood and Banno, 1973). From the Al/Cr ratios of spinels, the pressures for the Kutch xenoliths are suggested to be 12–15 kbar. If we integrate these data, it can be inferred that the Murud-Janjira granulites come from >30 km depth, close to the crust–mantle boundary. The seismic Moho in this region has been estimated at a depth of 31.5 km (Kaila *et al.*, 1981). The depth estimates therefore imply a lower crustal to transitional shallow mantle origin for the xenolith suite. The *P-T* array of Murud-Janjira granulites corresponds roughly to the higher side of the *P-T* array of Lesotho xenoliths (Griffin *et al.*, 1979). Temperatures of 800–900°C are common in similar suites of lower crustal xenoliths but the values are substantially higher than those defined by calculated conductive geotherms (Negi *et al.*, 1987), thereby indicating that the lithosphere

beneath Murud-Janjira was heated by intruding magmas.

Comparison with the heat flow data

The surface heat flow map of India (Ravi Shankar, 1988) shows a 'core zone' parallel to the west coast (Fig. 1) with high heat flow values of 100–180 mWm^{-2}, i.e. 3–4 times the average continental heat flow and is more than the upper limit of conductive heat flow (125 mWm^{-2}; Morgan, 1989). This narrow zone, extending from Cambay to Ratnagiri, is surrounded by a broad zone of decreasing heat flow extending across the Indian peninsula. Alkaline magmatism in the Deccan Flood Basalt Province occurred ~68 Ma ago (Venkatesan *et al.*, 1986; Basu *et al.*, 1993) and despite this fact, the geothermal gradient is high in comparison with the gradients in some contemporaneous alkali basalt provinces elsewhere in the world (Jones *et al.*, 1983). The high heat flow could be related to conductive and advective heat transfer from magmas that ponded at the crust-mantle boundary.

Implications for seismic data

Deep seismic sounding studies (Kaila *et al.*, 1981) along two E–W profiles (perpendicular to the west coast) in the vicinity of Bombay, have identified a 2 km thick low velocity layer at 35.5 km east of Bombay . In addition, three other reflectors are inferred at depths of 20, 25 and 30 km. The one at 25 km has been ascribed to the Conrad discontinuity (Kaila *et al.*, 1981). Our xenolith data permit interpretation of these reflectors as a transitional type of boundary layer between the lower crust and the intra- and under-plated layered ultramafites.

The discontinuity at 35.5 km to the east of Bombay shallows to 31.5 km near Bombay and to 21 km near Billimora (150 km north of Bombay). The area also coincides with a 300 km (N–S) × 60 km positive Bouger anomaly (Kaila *et al.*, 1981). This anomaly has been attributed to the Moho discontinuity (Kaila *et al.*, 1981, Kaila, 1988) which arches near Bombay. Recently Negi *et al.* (1986, 1987) have estimated the Curie depth of 43 km for this region and a lithospheric thickness of 101 km. These results are in agreement with those of Agarwal *et al.* (1992) who identified a magnetic interface at 40 ± 4 km. The geochemistry of xenoliths suggest that the crust-mantle boundary in this region is anomalous and metasomatized, which could account for low seismic velocities (e.g. O'Reilly and Griffin, 1985; O'Reilly *et al.*, 1990). The other factor responsible for the low velocity is the high temperature of this transitional crust-mantle boundary. The pressure range of 11–14 kbar indicated for the granulite xenoliths agrees approximately with the depth of the Moho, particularly because this region has been the focus of intense volcanism and as such, the petrological Moho may actually be deeper by 5–10 km (Kopylova *et al.*, 1995) than the crust-mantle boundary.

Conclusions

The lithospheric xenoliths from Murud-Janjira are mainly represented by pyroxenites and granulites. They have been derived from igneous protoliths that crystallized as cumulates of relatively primitive alkaline and sub-alkaline melts respectively, and therefore are not cogenetic with their host. The pyroxenites and the granulites formed from unrelated magmas, those of the pyroxenites being the more primitive. The xenoliths provide evidence of metasomatism which introduced phlogopite, sulphides and brought about LILE-enrichment in the protoliths.

The crust-mantle boundary beneath Murud-Janjira is transitional comprising garnet granulites interlayered with pyroxenites. The xenolith suite is lithologically diverse and is derived from this transitional boundary at depths of 30–40 km. The xenoliths suggest growth of continental lithosphere beneath Murud-Janjira by magmatic under-plating. Although the western Indian continental margin exhibits a high geothermal gradient from advective heat flow, the xenolith temperature estimates may represent the last metamorphic overprint possibly related to the Pan-African tectonothermal event. The metasomatized nature of the deep crust and a high geothermal gradient account for the low seismic velocities of the deep crust beneath the Deccan Traps.

Acknowledgements

We thank Hilary Downes for a critical review of the manuscript. Discussions with G. Sen and the late K.G. Cox were useful in preparing an initial draft of the paper. Constructive comments and suggestions by R. Vannucci and W.L. Griffin helped to improve the manuscript. Thanks are due to Goa University and the CNR-Centro per la Minerogenesi e la Geochimica Applicata of

Florence for providing laboratory facilities. Reviews by B.G.J. Upton and an anonymous reviewer are gratefully acknowledged.

References

Agarwal, B.N.P., Thakur, N.K. and Negi, J.G. (1992) Magsat data and Curie depth below Deccan flood basalts (India). *Pageoph.*, **138**, 678–91.

Auden, J.B. (1949) Dykes in Western India. A discussion of their relationship with Deccan Traps. *Trans. Nat. Inst. Sci. India.* **3**, 123–37.

Balasundaram, M.S. and Balasubramanyan, M.N. (1973) Geochronology of the Indian Precambrian. *Geol. Soc. Malaysia Bull.*, **6**, 213–26.

Basu, A.R. (1978) Trace elements and Sr – isotopes in some mantle derived hydrous minerals and their significance. *Geochim. Cosmochim. Acta*, **42**, 659–68.

Basu, A.R., Renne, P.R., Dasgupta, D.K., Teichmenn, F. and Poreda, R.G. (1993) Early and late alkali igneous pulses and a high ^{3}He plume origin for the Deccan Flood Basalts. *Science,* **261**, 902–6.

Best, M.G. (1975) Amphibole bearing cumulate inclusions, Grand Canyon, and their bearing on undersaturated hydrous magmas in the upper mantle. *J. Petrol.,* **16**, 212–36.

Boettcher, A.L. and O'Neil, J.R. (1980) Stable isotope, chemical and petrographical studies of high pressure amphiboles and micas: evidence for metasomatism in the mantle source regions of alkali basalts and kimberlites. *Amer. J. Sci.*, **280A**, 594–621.

Brandon, A.D. and Meen, J. K. (1995) Nd isotope evidence for the position of southernmost India terrains within East Gondwana. *Precamb. Res.*, **70**, 269–80.

Brown, G.M., Pinset, R.H., Coisy, P. (1980) The petrology of spinel peridotite xenoliths from Massif Central, France. *Amer. J. Sci.,* **280A**, 471–98.

Choudhary, A.K., Harris, N.B.W., van Calsteren, P. and Hawkesworth, C. J. (1992) Pan-African charnockite formation in Kerala, South India. *Geol. Mag.,* **129**, 257–64.

Courtillot, V.E., Feraud, G., Maluski, H., Vandamne, D., Moreau, M.G. and Besse, J. (1988) Deccan flood basalts and the Cretaceous-Tertiary boundary. *Nature,* **333**, 843–6.

Cox, K.G. (1983) The Deccan Traps and the Karoo: stragraphic implications of possible hot spot origins. *IAVCEI, Hamburg Meeting, Abstract vol.,* p. 96.

Cox, K.G. and Hawkesworth, C.J. (1985) Geochemical stratigraphy of the Deccan Traps at Mahableshwar, Western Ghats, India with implications for open system magmatic processes. *J. Petrol.,* **26**, 355–77.

Crawford, A.R. (1969) Reconnaissance Rb-Sr dating of the Precambrian rocks of the southern peninsular India. *J. Geol. Soc. Ind.*, **10**, 117–66.

Dessai, A.G. (1985) Ultramafic xenoliths(?) in lamprophyre dykes from Murud-Janjira, Raigarh district, Maharashtra. *Curr. Sci.,* **54**, 1235–8.

Dessai, A.G. (1987) Geochemistry and petrology of xenolith bearing alkaline lamprophyres from Murud-Janjira, Raigad district, Maharashtra. *J. Geol. Soc. Ind.,* **30**, 61–71.

Dessai, A.G. (1994) Magma fractionation and mixing in a nephelinite plug associated with Deccan magmatism at Murud-Janjira, south of Bombay. *J. Geol. Soc. Ind.*, **43**, 493–509.

Dessai, A.G. (1996) Geochemistry of the mantle beneath the Deccan Traps, south of Bombay. *Gondwana Geol. Mag. Spec. Vol.*, **2**, 201–12.

Dessai, A.G. and Bertrand, H. (1995) The 'Panvel Flexure' along the Western Indian continental margin: an extensional fault structure related to Deccan magmatism. *Tectonophys.*, **241**, 165–78.

Dessai, A.G. and Viegas, A.A.A.A. (1995) Multigeneration mafic dyke swarm related to Deccan magmatism, south of Bombay: implications on the evolution of the western continental margin. In *Dyke Swarms of Peninsular India* (T.C. Devaraju, ed.), Geol. Soc. Ind. Mem., **33**, 435–51.

Dessai, A.G., Rock, N.M.S., Griffin, B.J. and Gupta, D. (1990) Mineralogy and petrology of some xenolith bearing alkaline dykes associated with Deccan magmatism, south of Bombay, India. *Eur. J. Miner.*, **2**, 667–85.

Dewey, C.W. and Stephens, W.E. (1992) Deccan related magmatism west of Seychelles-India rift. In *Magmatism and the causes of continental break-up* (B.C. Storey, T. Alabaster and R.J. Pankhurst, eds), *Geol. Soc. Lond. Spec. Publ.*, **68**, 271–91.

Downes, H. (1993) The nature of the lower continental crust of Europe: petrological and geochemical evidence from xenoliths. *Phys. Earth Planet. Inter.*, 79, 195–218.

Droop, G.T.R. (1987) A general equation for estimating Fe^{3+} concentrations in ferromegnesian silicates and oxides from microprobe analysis using stoichiometric criteria. *Mineral. Mag.,* **51**, 431–5.

Duncan, R.A. and Pyle, D.G. (1988) Rapid eruption of Deccan flood basalts, western India. In *Deccan Flood Basalts* (K.V. Subbarao, ed.), *Mem. Geol. Soc. Ind.*, **10**, 1–9.

Edgar, A.D. (1987) The genesis of alkaline magmas with emphasis on their source region: inferences from experimental studies. In *Alkaline Igneous Rocks.* (B.G.J. Upton, ed.), Geol. Soc. Lond., Spec. Publ., **30**, 29–52.

Frey, F.A. and Green, D.H. (1974) The mineralogy, geochemistry and origin of lherzolite inclusions in Victorian basanites. *Geochim. Cosmochim. Acta,* **38**,

1023–59.

Frey, F.A. and Prinz, M. (1978) Ultramafic inclusions from San Carlos Arizona: petrologic and geochemical data bearing on their petrogenesis. *Earth Planet. Sci. Lett.*, **38**, 129–76.

Griffin, W.L. and O'Reilly, S.Y. (1987) Is the continental Moho the crust-mantle boundary? *Geology*, **15**, 241–4.

Griffin, W.L., Carswell, D.A. and Nixon, P.H. (1979) Lower crustal granulites from Lesotho, South Africa. In *The mantle sample: inclusions in kimberlites and other volcanics* (F.R. Boyd and H.O.A. Meyer, eds), Proc. 2nd Int. Kimberlite Conf., American Geophysical Union, Washington, D.C., pp. 59–86.

Halliday, A.N., Dickin, A.P., Hunter, R.H., Davis, G.R., Dempster, T.J., Hamilton, P.J. and Upton, B.G.J. (1993) Formation and composition of the lower continental crust evidence from a Scottish xenolith suite. *J. Geophys. Res.*, **98(B1)**, 581–607.

Hansen, E.C., Hickman, N.H., Grant, N.K. and Newton, R.C. (1985) Pan-African age of 'Peninsular Gneiss' near Madurai, south India. (Abst.) EOS (Trans. Amer. Geophys. Union), **66,** 419–20.

Harris, N.B.W. and Santosh, M. (1993) Geochronological constraints on granulite formation in southern India and Sri Lanka. *Geol. Soc. Ind. Mem.*, **25**, 361–79.

Harte, B. (1983) Mantle peridotites and processes – the kimberlite sample. In *Continental basalts and mantle xenoliths* (C.J. Hawkesworth and M.J. Norry eds), Shiva Publishing Ltd., Nantwich, UK, pp. 46–91.

Holmes, A. (1965) *Principles of Physical Geology.* Thomas Nelson and Sons, London, 1288 p.

Hooper, P.R. (1990) The timing of crustal extension and the eruption of continental flood basalts. *Nature*, **345**, 246–249

Irving, A.J. (1974) Pyroxene-rich ultramafic xenoliths in the Newer Basalts of Victoria, Australia. *Neus Jahrb. Mineral. Abh.*, **120**, 147–67.

Irving, A.J. (1980) Petrology and geochemistry of composite xenoliths in alkali basalts and implications for magmatic processes within the mantle. *Amer. J. Sci.*, **280A**, 389–426.

IUGS Subcommission on the systematics of igneous rocks (1973) Plutonic rocks: classification and nomenclature. *Geotimes*, **18**, 26–30.

Jones, A.P., Smith, J.V., Dawson, J.B. and Hansen, E.C. (1983) Metamorphism, partial melting and K metasomatism of garnet-scapolite-kyanite granulite xenoliths from Lashaine, Tanzania. *J. Geol.*, **91**, 143–65.

Kaila, K.L. (1988) Mapping the thickness of Deccan Trap flows in India from DSS studies and inferences about a hidden Mesozoic basin in the Narmada-Tapti region. In *Deccan Flood Basalts* (K.V. Subbarao, ed.), Mem. Geol. Soc. Ind., **10**, 91–116.

Kaila, K.L., Murthy, P.R.K., Rao, V.K. and Kharatchko, G.E. (1981) Crustal structure from deep seismic sounding along Koyna II (Kelsi-Loni) profile in the Deccan Trap India. *Tectonophys.*, **73**, 365–84.

Kempton, P.D., Downes, H., Sharkov, E.V., Vetrin, V.R., Ionov, D.A., Carswell, D.A. and Beard, A. (1995) Petrology and geochemistry of xenoliths from the northern Baltic shield: evidence for partial melting and metasomatism in the lower crust beneath an Archaean terraine. *Lithos*, **36**, 157–84.

Kempton, P.D., Downes, H. and Embey-Isztin, A. (1997) Mafic granulite xenoliths in Neogene alkali basalts from the western Pannonian basin: insight into the lower crust of a collapsed orogen *J. Petrol.*, **38**, 941–70.

Kopylova, M.G., O'Reilly, S.Y. and Genshaft, Yu. S. (1995) Thermal state of the lithosphere beneath central Mongolia: evidence from deep seated xenoliths from Shavaryn-Saram volcanic centre in the Tariat depression, Hangai, Mongolia. *Lithos*, **36**, 243–255.

Krishnamurthy, P., Pande, K., Gopalan, K. and MacDougall, J.D. (1988) Upper mantle xenoliths in alkali basalts related to Deccan Trap volcanism. In *Deccan Flood Basalts* (K.V. Subbarao, ed.), Mem. Geol. Soc. Ind., **10**, 53–67.

Kroner, A. (1981) Precambrian plate tectonics. In *Precambrian Plate Tectonics* (A. Kroner, ed.) Elsevier Amsterdam, pp. 57–90.

Kuno, H. and Aoki, K. (1970) Geochemistry of ultramafic nodules and their bearing on the origin of basaltic magmas. *Phys. Earth Planet. Interior*, **3**, 273–301.

Le Maitre, R.W. (1976) Some problems of the projection of chemical data into mineralogical classification. *Contrib. Mineral. Petrol.*, **56**, 181–9.

Mahoney, J.J. (1988) Deccan Traps. In *Continental Flood Basalts* (J.D. MacDougall, ed.), Kluwer, Dordrecht, Netherlands, 151–94.

Mahoney, J.J., MacDougall, J.D., Lugmair, G.W., Gopalan, K. and Krishnamurthy, P. (1985) Origin of contemporaneous tholeiite and K–rich alkali lavas; a case study from the northern Deccan Plateau India. *Earth Planet. Sci. Lett.*, **72**, 39–53.

Menzies, M. and Murthy, V.R. (1980) Nd and Sr isotope geochemistry of hydrous mantle nodules and their host alkali basalts: implications for local heterogeneities in metasomatically veined mantle. *Earth Planet. Sci. Lett.*, **46**, 323–34.

Mercier, J.C.C. (1980) Single pyroxene thermobarometry. *Tectonophys.*, **70**, 1–37.

Mercier, J.C.C. and Nicholas, A. (1975) Textures and fabrics of upper mantle peridotites as illustrated by xenoliths from basalts. *J. Petrol.*, **16**, 454–87.

Mitchell, R.H. (1986) *Kimberlites: Mineralogy, Geochemistry and Petrology.* Plenum Press, New

York, 442 p.

Morgan, P. (1989) Heat flow in the Earth. In *The Encyclopaedia of Solid Earth Geophysics* (E.D. James, ed.), Van-Nostrand Rheinhold Co., New York, pp. 624–46.

Morgan, W.J. (1981) Hot-spot tracks and the opening of Atlantic and Indian oceans. In *The Sea* (C. Emiliani, ed.), Wiley Interscience, New York, **7**, 443–87.

Morimoto, M., and eight others (1988) Nomenclature of pyroxenes. *Mineral. Mag.*, **52**, 535–50.

Mottana, A. (1986) Crystal chemical evaluation of garnet and omphacite microprobe analysis: its bearing on the classification of eclogites. *Lithos*, **19**, 171–86.

Negi, J.G., Pandey, O.P. and Agarwal, P.K. (1986) Supermobility of hot Indian lithosphere. *Tectonophys.*, **131**, 147–56.

Negi, J.G., Agarwal, P.K. and Pandey, C.P. (1987) Large variation in Curie depth and lithospheric thickness beneath the Indian subcontinent and case for magnetothermometry. *Geophys. J. R. Astron. Soc.*, **88**, 763–75.

Newton, R.C. and Perkins, D. (1982) Thermodynamic calibration of geothermometers based on the assemblage garnet-plagioclase-orthopyroxene (clinopyroxene)-quartz. *Amer. Mineral.*, **67**, 203–22.

O'Reilly, S.Y. and Griffin, W.L. (1985) A xenolith-derived geotherm for southeastern Australia and its geophysical implications. *Tectonophys.*, **111**, 41–63.

O'Reilly, S.Y. and Griffin, W.L. (1987) Eastern Australia: 4000 km of mantle samples. In *Mantle Xenoliths* (P.H. Nixon, ed.), Wiley, London, pp. 267–80.

O'Reilly, S.Y. and Griffin, W.L. (1995) Moho and petrologic crust-mantle boundary coincide under southeastern Australia. Comment. *Geology*, **22**, 666–7.

O'Reilly, S.Y., Jackson, I. and Bezant, C. (1990) Seismic and thermal parameters of upper mantle rocks from eastern Australia: implications of seismic modelling. *Tectonophys.*, **185**, 67–82.

O'Reilly, S.Y., Nicholls, I.A. and Griffin, W.L. (1989) Xenoliths and megacrysts of mantle origin. In *Intraplate Volcanism in Eastern Australia and New Zealand* (R.W. Johnson, ed.), 408 p.

Peng, Z.G., Mahoney, J., Hooper, P., Harris, C. and Bean, J. (1994) A role for lower continental crust in flood basalt genesis? Isotopic and incompatible element study of lower six formations of the western Deccan Traps. *Geochim. Cosmochim. Acta*, **58**, 267–88.

Powell, R. and Holland, T.J.B. (1988) An internally consistent data set with uncertainties and correlations: 3. Applications to geobarometry, worked examples and a computer programme. *J. Metam. Geol.*, **6**, 173–204.

Ravi Shanker (1988) Heat flow map of India and discussion on its geological and economic significance. *Indian Minerals*, **42**, 89–110.

Richards, M.A., Duncan, R.A. and Courtillot, V. (1989) Flood basalts and hot spot tracks: Plume heads and tails. *Science*, **246**, 103–7.

Rogers, N.W. (1977) Granulite xenoliths from Lesotho kimberlite and the lower continental crust. *Nature*, **270**, 681–4.

Rudnick, R.L. (1992) Xenolith-samples of the lower continental crust. In *The Continental Crust* (D.M. Fountain, R.J. Arculus and R.W. Kay, eds) Elsevier, New York, pp. 269–316.

Santosh, M., Kamagi, H., Yoshida, M. and Nanda-Kumar, V. (1992) Pan-African charnockite formation in East Gondwana: geochronology (Sm-Nd and Rb-Sr) and petrogenetic constraints. *Bull. Int. Geol. Assoc.*, **25**, 1–10.

Sen, G. (1988) Petrogenesis of spinel lherzolite and pyroxenite suite xenoliths from the Koolau shield, Oahu Hawaii: Implications for petrology of the post-eruptive lithosphere beneath Oahu. *Contrib. Mineral. Petrol.*, **100**, 61–91.

Stosch, H.G., Kugmair, G.W. and Kovalenko, V.I. (1986) Spinel peridotite xenoliths from Tariat depression, Mongolia II, geochemical and Nd-and Sr-isotopic composition and their implications for the evolution of the subcontinental lithosphere. *Geochim. Cosmochim. Acta*, **50**, 2601–14.

Stosch, H.G., Ionov, D.A., Puchtel, I.S., Galer, S.J.G. and Sharpouri, A. (1995) Lower crustal xenoliths from Mongolia and their bearing on the nature of the deep crust beneath central Asia. *Lithos*, **36**, 227–42.

Subbarao, K.V. and Hooper, P.R. (1988) Reconnaissance map of the Deccan Basalt Group in the Western Ghats, India. In *Deccan Flood Basalts* (K.V. Subbarao, ed.), Mem. Geol. Soc. Ind., **10**, (enclosure).

Sun, S.S. (1980) Lead isotopic study of young volcanic rocks from mid-oceanic ridges, oceanic islands and island-arcs. *Phil. Trans. R. Soc. Lond.*, **A297**, 409–45.

Sun, S.S. and McDonough, W.F. (1989) Chemical and isotopic systematics of oceanic basalts: implications for mantle composition and processes. In *Magmatism in ocean basins* (A.D. Saunders and M.J. Norry, eds), *Geol. Soc. Lond. Spec. Publ.*, **42**, 313–45.

Szabo, C.S. and Taylor, L.A. (1994) Mantle petrology and geochemistry beneath the Nograd-Gomer volcanic field, Carpathian-Pannonian region. *Inter. Geol. Rev.*, **36**, 328–58.

Taylor, S.R. and McLennan, S.M. (1985) *The continental crust: its composition and evolution.* Blackwell, Oxford, 312 p.

Vaselli, O., Downes, H., Thirlwall, M., Dobosi, G., Coradossi, N., Seghedi, I., Szakacs, A. and Vannucci, R. (1995) Ultramafic xenoliths in Plio-Pleistocene alkali basalts from the eastern Transylvanian basin: depleted mantle enriched by vein metasomatism. *J. Petrol.*, **36**, 23–53.

Venkatesan, T.R., Pande, K. and Gopalan, K. (1986) $^{40}Ar-^{39}Ar$ dating of Deccan basalts. *J. Geol. Soc. Ind.*, **27**, 102–09.

Watts, A.B. and Cox, K.G. (1989) The Deccan Trap: an interpretation in terms of progressive lithospheric flexure in response to a migrating load. *Earth Planet. Sci. Lett.*, **93**, 85–97.

Wells, P.R.A. (1977) Pyroxene thermometry in simple and complex systems. *Contrib. Mineral. Petrol.*, **62**, 129–39.

Wilson, M. (1989) *Igneous Petrogenesis: A Global Tectonic Approach.* Unwin Hyman, London 446 p.

Wilshire, H.G. and Shervais, J.W. (1975) Al-augite and Cr-diopside ultramafic xenoliths in basaltic rocks from Western United States. In *Physics and Chemistry of the Earth,* (L.H. Aherns, J.B. Dawson, A.R. Duncan and A.J. Erlank, eds) Pergamon Press, New York, **9**, 257–72.

Witt-Eickschen, G., Seck, H.A. and Reys, C.H. (1993) Multiple enrichment processes and their relationship in the subcrustal lithosphere beneath the Eifel (Germany). *J. Petrol.*, **34**, 1–22.

Wood, B.J. and Banno, S. (1973) Garnet-orthopyroxene and orthopyroxene-clinopyroxene relationships in simple and complex systems. *Contrib. Mineral. Petrol.*, **42**, 109–12.

[*Manuscript received 22 June 1998: revised 24 November 1998*]

Appendix I: Petrographic features of Murud-Janjira xenoliths

Modal proportions of the minerals were estimated with a James Swift automatic point counter. Abbreviations: cpx – clinopyroxene, opx – orthopyroxene, gnt – garnet, plg – plagioclase, phlg – phlogopite, ap – apatite, rt – rutile, mt – magnetite, spnl – spinel, sph – sphene, cc – calcite, scp – scapolite, opq – opaque, tr – trace.

Clinopyroxenites

281X. Coarse grained clinopyroxenite (91% cpx + 9% opq). Glass green subhedral diopside with slightly darker borders with rare exsolution blebs of opx.

281VII. Medium grained phlogopite clinopyroxenite (81% cpx + 11% phlg + 8% opq +tr opx). Pale green cpx. Rare interstitial opx. Intergranular phlg strongly pleochroic from dark brown to pale yellowish brown.

281S. Coarse grained clinopyroxenite (89% cpx + 11% opq). Anhedral pale green cpx contains abundant fluid/melt inclusions.

Granulites/eclogitic granulites

267RHA. Medium grained granulite (30% plg + 22% mt + 48% rt + tr cpx). Weak discontinuous banding of plg alternating with opq + rt + cpx. Cpx pale green. Plg rarely pseudomorphed by cc shows preferred orientation.

281C1. Medium grained garnet granulite (52% cpx + 46% pgl + 2% gnt). Porphyroclastic to meta-igneous texture appears to be cumulate. Cpx deep green in colour, plg shows preferred orientation suggesting original igneous layering. Gnt pale pink, altered along rims to kelyphite. Aggregates of granular sph around gnt.

281VI. Medium grained garnet granulite (53% cpx + 31% pgl + 15% gnt + tr opx, opq) equant granoblastic. Cpx pale green, gnt pale pink altered along rims to kelyphite; inner rim pale brown fibrous or acicular, outer one vermicular with opq oxides. Gnt with cpx inclusions and also veined by it.

281P. Medium grained garnet granulite (81% cpx + 16% gnt + 3% plg + tr phlg). Cpx pale green, gnt with rims of kelyphite, plg stumpy, phlg anhedral, intergranular.

281V. Medium grained eclogitic granulite (58% cpx + 33% gnt + 9% phlg). Massive. Cpx darker green, gnt pale pink with cpx inclusions and rt exsolutions. Phlg intergranular partially replaces cpx.

Composite xenolith

281W. Medium grained garnet granulite (51% cpx + 28% gnt + 18% opq + 2% plg + tr opx, ap) and medium grained clinopyroxenite (95% cpx + 5% opq). Granulite is foliated and banded. Layering on mm scale defined by alternating plg-rich and cpx+gnt-rich bands. Preferred orientation of elongated cpx defines foliation. Plg veins cut across foliation. Cpx contains fluid/melt inclusions. Gnt pale pink is altered with double rims of kelyphite. Pyroxenite consists of anhedral pale green cpx and opq. Contact between

the two lithologies marked by phlg which decreases away from the contact.

Fragmented xenoliths

281A, B, D and E. Coarse grained fragmented clinopyroxenite. Aggregates of few grains of pale green cpx and a couple of opq.

281C. Medium grained clinopyroxenite (reacted). Aggregate of few grains of cpx + opq. Opx and spnl occur in melt pockets.

281G. Medium grained granulite (reacted). Aggregate of few grains of cpx + plg + phlg. Spnl reacted with melt to form opq oxides.